Applied Thermal Engineering 98 (2016) 330–339

Contents lists available at ScienceDirect

Applied Thermal Engineering

journal homepage: www.elsevier.com/locate/apthermeng

Research Paper

Evaluation of R448A and R450A as low-GWP alternatives for R404A and R134a using a micro-fin tube evaporator model

Juan Manuel Mendoza-Miranda [a], Adrián Mota-Babiloni [b,c,*], Joaquín Navarro-Esbrí [c]

[a] Interdisciplinary Professional Unit of Engineering Campus Guanajuato, National Institute Polytechnic, Av. Mineral de Valenciana 200 Fracc. Industrial Puerto Interior, C.P. 36275, Silao de la Victoria, Guanajuato, Mexico
[b] Institute for Industrial, Radiophysical and Environmental Safety (ISIRYM), Camino de Vera s/n, Polytechnic University of Valencia, E46022, Valencia, Spain
[c] ISTENER Research Group, Department of Mechanical Engineering and Construction, Campus de Riu Sec s/n, University Jaume I, E12071, Castellón de la Plana, Spain

HIGHLIGHTS

- Different correlations for flow boiling in microfin tubes are evaluated.
- Akhavan-Behabadi et al. correlation presents the best predictions.
- Min. and max. deviations occur with R134a and R450A, respectively.
- R450A and R134a evaporator performances are almost the same.
- Due to high R448A glide, its evaporator performance is very different from R404A.

ARTICLE INFO

Article history:
Received 9 June 2015
Accepted 13 December 2015
Available online 30 December 2015

Keywords:
R134a
R450A
R448A
R404A
Flow boiling heat transfer correlations
Evaporator model

ABSTRACT

When retrofitting new refrigerants in an existing vapour compression system, their adaptation to the heat exchangers is a major concern. R450A and R448A are commercial non-flammable mixtures with low GWP developed to replace the HFCs R134a and R404A, fluids with high GWP values. In this work the evaporator performance is evaluated through a shell-and-microfin tube evaporator model using R450A, R448A, R134a and R404A. The accuracy of the model is first studied considering different recently developed micro-fin tube correlations for flow boiling phenomena. The model is validated using experimental data from tests carried out in a fully monitored vapour compression plant at different refrigeration operating conditions. The main predicted operational parameters such as evaporating pressure, UA_{TP}, and cooling capacity, when compared with experimental data, fit within ±10% using the Akhavan-Behabadi et al. correlation for flow boiling. Results show that R450A and R404A are the refrigerants in which the model fits better, even though R448A and R134a predictions are also accurate.

1. Introduction

During the past decades, R134a, R404A and R507A have being used in different refrigeration and air conditioning applications as non-ozone depleting R12 [1] and R22 [2] substitutes, respectively. They present good energy performance, are non-toxic and non-flammable. However, due to the Kyoto Protocol approval [3], they have been identified as greenhouse gas (GHG) as the rest of HFCs (hydrofluorocarbon).

In order to enforce that agreed at the Kyoto Protocol, the European Union approved the Directive 2006/40/EC in 2006 [4], also known as F-gas Regulation. This Directive affected refrigerants with a GWP (Global Warming Potential) higher than 150 in new vehicles from 2011 and in all new vehicles produced from 2017. Then, in 2014, the Directive 2006/40/EC has been replaced by the Regulation (EU) No 517/2014, which bans the use of HFC with high GWP values in the rest of the refrigeration and air conditioning systems [5].

Considering the very large refrigeration applications using the vapour compression system, several low GWP refrigerant fluids with different characteristics can be found to replace HFCs in vapour compression systems, both natural and synthetic [6]. Natural refrigerants comprise hydrocarbons, flammable but economical and energy efficient; carbon dioxide, increasingly relevant and used in transcritical or cascade systems; and ammonia, toxic and flammable but very efficient. Synthetic refrigerants are considered good low and mid-term alternatives and can be differentiated as low-GWP HFCs, HFOs (hydrofluoroolefines) or mixtures of both groups.

Two HFOs appeared as R134a replacements [7]: R1234yf [8] and R1234ze(E) [9]. They present low-flammability, they are non-toxic

Abbreviations: GHG, greenhouse gas; GWP, global warming potential; HFC, hydrofluorocarbon; HFO, hydrofluoroolefines; HTC, heat transfer coefficient; ODP, ozone depletion potential.

* Corresponding author. Tel.: +34 964387529; fax: +34 964728106.
E-mail address: admoba@upv.es (A. Mota-Babiloni).

http://dx.doi.org/10.1016/j.applthermaleng.2015.12.064
1359-4311/

Table 1
Refrigerants' main properties [30].

	R134a	R450A	R404A	R448A
ASHRAE safety classification	A1	A1	A1	A1
ODP	0	0	0	0
100-year GWP	1430	547	3922	1273
Critical temperature (K)	374.21	379.02	345.20	356.81
Critical pressure (kPa)	4059.28	3814	3728.85	4674.93
NBP (K)	247.08	521.20	227.41	233.05
Glide[a] (K)	-	0.78	0.75	6.27
Liquid density[a] (kg m^{-3})	1295.27	1253.28	1150.59	1192.39
Vapour density[a] (kg m^{-3})	14.35	13.93	30.32	22.09
Liquid c_p[a] (kJ kg^{-1} K^{-1})	1.34	1.32	1.39	1.42
Vapour c_p[a] (kJ kg^{-1} K^{-1})	0.90	0.89	1.00	0.98
Liquid therm. cond.[a] (W m^{-1} K^{-1})	$92.08 \cdot 10^{-3}$	$83.09 \cdot 10^{-3}$	$73.15 \cdot 10^{-3}$	$92.41 \cdot 10^{-3}$
Vapour therm. cond.[a] (W m^{-1} K^{-1})	$11.50 \cdot 10^{-3}$	$11.57 \cdot 10^{-3}$	$12.82 \cdot 10^{-3}$	$12.01 \cdot 10^{-3}$
Liquid viscosity[a] (Pa s^{-1})	$267.04 \cdot 10^{-6}$	$258.22 \cdot 10^{-6}$	$179.70 \cdot 10^{-6}$	$188.35 \cdot 10^{-6}$
Vapour viscosity[a] (Pa s^{-1})	$10.72 \cdot 10^{-6}$	$11.15 \cdot 10^{-6}$	$11.00 \cdot 10^{-6}$	$11.42 \cdot 10^{-6}$

[a] Temperature = 273 K.

and their GWP values are 4 and 6 (accomplishing GWP limitations), respectively. R1234yf has been proposed as a R134a drop-in substitute in mobile air conditioning applications [10], and R1234ze(E) can be used in chillers [11] and heat pumps [12], among other applications.

Although R1234ze(E) shows relevant advantages in refrigeration systems, its use as a R134a drop-in replacement is not recommended because it presents lower cooling capacity [13] and low-flammability [14]. With the purpose of finding a most satisfactory solution (non-flammable, lower GWP values, with acceptable cooling capacity) and extending the lower GWP refrigerant usage for substitution of another HFC (as R404A and R410A), it has been mixed with some HFCs [15].

In this way, blends like R444A, R445A and R450A appeared as alternatives to substitute the refrigerant R134a. Focusing on blend R450A, it is a mixture of R1234ze(E) and R134a (58/42 in % mass) intended to replace R134a in medium temperature applications (chillers, heat pumps and commercial refrigeration, among others) [16]. It is non-flammable and its GWP is 549 (though it is not low enough for some cooling systems in Europe). It has shown good efficiency compared to R134a, as demonstrated by Mota-Babiloni et al. [17] in a vapour compression test rig and Tewis Smart solutions [18] or Honeywell International Inc [19] in a supermarket cascade systems. Lower performance has been shown in a water-cooled screw chiller installation [20].

In the other way, R448A appears as a blend alternative to substitute the R404A and it is composed of R32/R125/R134a/R1234yf/R1234ze(E) (26/26/20/21/7 in % mass), resulting non-flammable and GWP of 1205. R448A can substitute R404A in large centralized systems at low and medium evaporating conditions [21]. As happens for R450A, this HFO/HFC mixture also presents good performance. Mota-Babiloni et al. [22] studied theoretically six R404A alternatives in four vapour compression configurations, obtaining high efficiency simulating with R448A. Yana Motta et al. [23], using a 2.2 kW semi-hermetic condensing unit with evaporator for walk-in freezer/cooler, show that R448A matches the capacity of R404A with 6% higher efficiency. Rajendran [24] obtained lower energy consumption for R448A (3% to 8%) in a scroll compressor centralized Direct Expansion system with cases and food simulators. Abdelaziz and Fricke [25], in a test facility that uses reciprocating compressors and two separate temperature/humidity controlled rooms, found that refrigerant R448A average energy efficiency was 11.6% higher than that obtained with R404A.

When designing vapour compression systems, the evaporator selection is one of the most important parts [26]. One of the main parameters in an evaporator design is the flow boiling heat transfer coefficient (HTC) and depends on the evaporator geometry and the refrigerant properties [27]. Flow boiling HTC can be determined accurately through steady-state evaporator models, as demonstrated, for example, by Navarro-Esbrí et al. [28] or Zhao et al. [29] for R1234yf and R134a.

R450A and R448A are promising alternatives to two of most currently used refrigerants, R134a and R404A, due to their similar properties (Table 1). The problem is that the there are few data available for both alternative refrigerants and the effect of replacing HFCs cannot be predicted properly. In this paper a shell-and-micro-fin tube evaporator model is validated and used to evaluate these refrigerants considering different relevant heat exchanger parameters. The most accurate model is applied to compare the evaporator performance between these refrigerants. The conclusions of this work can be used in the evaluation of HFC substitution or in the refrigeration system and heat exchanger design using R450A and R448A, two refrigerants that can achieve great GWP reductions and, therefore, lessen the global warming.

The rest of the paper is structured as follows: In section 2, the experimental setup, refrigerants and test performed are presented. In section 3, the evaporator model is mentioned. In section 4, the correlations selected are exposed. In section 5, the results of the study are discussed. Finally, in section 6, the main conclusions are summarized.

2. Experimental setup

2.1. Test bench

The test bench used in this work is a fully monitored vapour compression plant that consists of a main circuit and two secondary circuits (Fig. 1). The vapour compression system is composed of the following components:

- Reciprocating open compressor, driven by variable-speed 7.5 kW electric motor using polyolester (POE) oil as lubricant. The compressor speed can be selected using an inverter.
- Shell-and-smooth tube condenser (1–2), with refrigerant flowing along the shell and the water (used as secondary fluid) inside the tubes.
- Shell-and-micro-fin tube evaporator (1–2), where the refrigerant flows inside the tubes and a water/propylene glycol mixture (65/35 by volume) along the shell.
- Thermostatic expansion valve.
- Corrugated counterflow tube-in-tube internal heat exchanger (also known as suction-line/liquid-line heat exchanger), which is activated or deactivated by a set of solenoid valves.

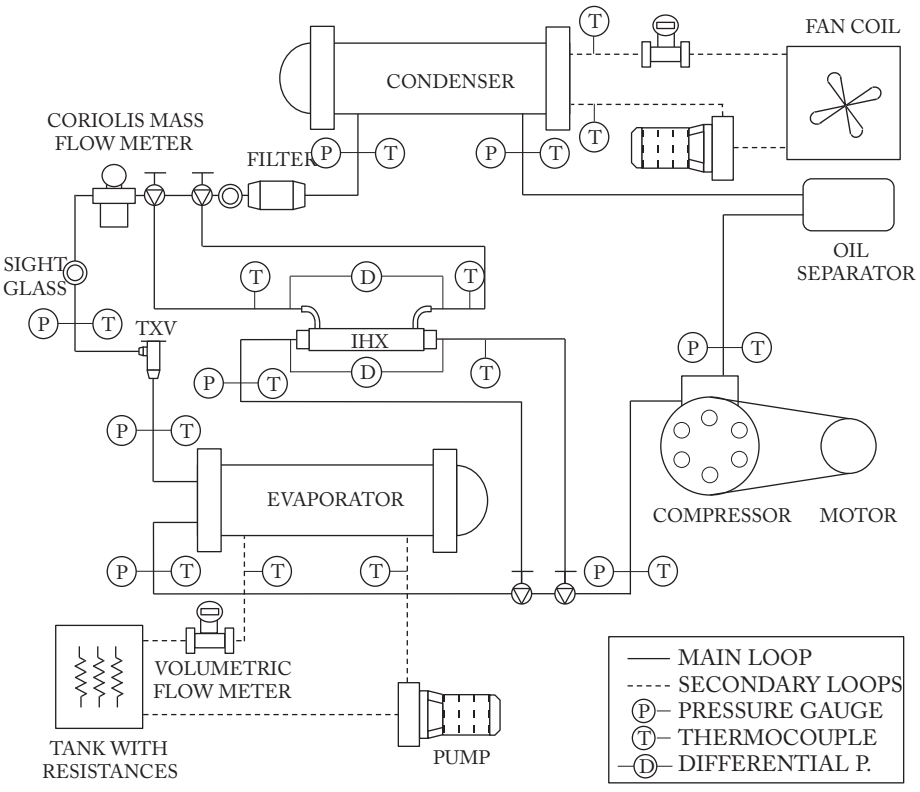

Fig. 1. Test bench schematic diagram.

The secondary circuits fix the requested evaporating and condensing conditions:

- The heat removal circuit is formed of a heat load circuit that is composed of a set of immersed electrical resistances regulated by a Proportional Integral Derivative (PID) controller.
- The heat removal circuit uses a fan and an auxiliary chiller.
- In both circuits the secondary fluid flow rate can be adjusted using a variable-speed pump.

The main characteristics of the evaporator (and micro-fin tube) geometry are listed in Table 2.

As mentioned before the test bench is completely monitored to obtain the main thermodynamic parameters (through temperature and pressure measurements) at the inlet and outlet of each main component (the location of sensors can be seen in Fig. 1). The system also contains a Coriolis flow meter in the main circuit and two electromagnetic flow meters in the secondary circuits. The compressor power consumption and rotation speed are also measured for energetic calculations. Detailed information about sensors is listed in Table 3.

Finally, all data generated by all sensors were gathered by a data acquisition system (every 0.5 seconds) and monitored and stored using a PC. The refrigerant thermodynamic states are calculated from the REFPROP v9.1 database [30].

Table 2
Evaporator geometry.

Total number of tubes	76
Number of tube passes	2
Number of shell passes	1
Inner tube diameter (m)	0.00822
Outside tube diameter (m)	0.00952
Number of micro-fins	30
Fin height (m)	$2{\cdot}10^{-4}$
Helix angle (°)	18
Inner shell diameter (m)	0.131
Tube length (m)	0.8182
Transverse tube spacing (m)	0.01142
Clearance between tubes (m)	0.0019
Number of baffles	5
Tube material	Copper

Table 3
Summary of sensors and their uncertainty associated.

Measured parameters	Sensor installed	Uncertainty
Temperatures	K-type thermocouples	±0.3K
Pressures	Piezoelectric pressure transducers	±7 kPa
Mass flow rate	Coriolis mass flow meter	±0.22%
Volumetric flow rate	Electromagnetic flow meter	±0.25%
Compressor power consumption	Digital wattmeter	±0.15%
Compressor rotation speed	Capacitive sensor	±1%

2.2. Tests performed

The tests conditions cover a complete mid (all refrigerants) and low (R448A and R404A) evaporation temperature range of vapour compression systems (Table 4).

The evaporating pressure is defined considering glide effects on heat exchangers, Eq. (1) is applied to correct R450A and R448A evaporating pressure [15,22].

$$P_{evap} = \frac{1}{3}P_{bubble} + \frac{2}{3}P_{dew} \quad (1)$$

Table 4
Test conditions (min–max).

	R134a	R450A	R404A	R448A
Evaporation pressure (kPa)	175.8–375.2	163.9–350.9	162.6–418.3	132.5–401.2
Refrigerant mass flow rate (kg s^{-1})	0.031–0.086	0.029–0.085	0.021–0.096	0.009–0.075
Refrigerant quality at the evaporator inlet	0.19–0.43	0.21–0.47	0.25–0.58	0.23–0.46
Refrigerant superheat at the evaporator exit (K)	5.6–9.8	6.5–10.2	5.5–13.5	9.7–11.8
Brine propylene glycol inlet temperature (K)	264.8–293.4	270.2–305.0	250.3290.9	250.43–287.88
Brine propylene glycol outlet temperature (K)	263.9–290.6	268.5–296.3	248.3–285.0	248.98–287.25
Secondary fluid volumetric flow rate (m^3 h^{-1})	1.14–1.24	1.17–1.27	1.02–1.82	1.09–1.83

3. Evaporator model

The model is based on the thermal analysis ε-NTU method, correlations are used to determine convective heat transfer coefficients and the data are provided by the evaporator manufacturer (Table 2). The evaporator is modeled by dividing it into two zones that correspond to the state of the refrigerant, i.e., evaporation and superheating zones. The complete evaporator model (development, assumptions, and equations, etc.) is explained and analysed in Mendoza-Miranda et al. [31]. The overall heat transfer coefficient is calculated using Eq. (2), which includes the thermal resistance associated with the fouling on the shell side, $R_{o,e}$. This value is 0.000086 m^2 K W^{-1} for water/propylene-glycol brine containing below 40% of propylene glycol according to the manufacturer data.

$$U_{zone}=\left[\left(\frac{1}{\alpha_{i,zone}}\right)\left(\frac{d_o}{d_i}\right)+R_{o,e}+\frac{d_o\ln\left(\frac{d_o}{d_i}\right)}{2k}+\frac{1}{\alpha_{o,brine}}\right]^{-1} \tag{2}$$

The internal heat transfer coefficient, $\alpha_{i,zone}$, in single phase for turbulent flow for micro-fin tubes is given by the Jensen and Vlakancic correlation [32] defined as

$$\alpha_i=\left(\frac{k}{d_i}\right)F_1^{-0.5}F_2\left(\frac{0.25\pi d_i^2}{0.25\pi d_i^2-N_f\cdot e\cdot t}\right)^{0.8}\mathrm{Nu}_s \tag{3}$$

$$F_1=\begin{cases}1-1.577\left(\frac{N_f\sin\beta}{\pi}\right)^{0.64}\left(\frac{2e}{d_i}\right)^{0.53}\left[\left(\frac{\pi}{N_f}-\frac{t}{d_i}\right)\cos\beta\right]^{0.28} & e/d_i\le 0.02\\ 1-0.994\left(\frac{N_f\sin\beta}{\pi}\right)^{0.89}\left(\frac{2e}{d_i}\right)^{0.44}\left[\left(\frac{\pi}{N_f}-\frac{t}{d_i}\right)\cos\beta\right]^{0.41} & 0.02<e/d_i\le 0.03\end{cases} \tag{4}$$

$$F_2=\left(1+\frac{2N_f\cdot e}{\pi d_i}\right)\left(1-0.059\left(\frac{N_f\sin\beta}{\pi}\right)^{-0.31}\left[\left(\frac{\pi}{N_f}-\frac{t}{d_i}\right)\cos\beta\right]^{-0.66}\right) \tag{5}$$

where Nu_s is obtained from the Gnielinskis' correlation [33] for a smooth tube defined as

$$\mathrm{Nu}_s=\frac{(f/2)(\mathrm{Re}-1000)\mathrm{Pr}}{1+12.7(f/2)^{1/2}(\mathrm{Pr}^{2/3}-1)} \tag{6}$$

where

$$f=[1.58\ln(\mathrm{Re})-3.28]^{-2} \tag{7}$$

For the external forced convection on the array of tubes the Zhukauskas correlation [34], Eq. (8), is used.

$$\alpha_{o,brine}=C\,\mathrm{Re}^m\,\mathrm{Pr}^{0.36}\left(\frac{\mathrm{Pr}}{\mathrm{Pr}_w}\right)^{1/4}\left(\frac{k_f}{d_o}\right) \tag{8}$$

where coefficients, C and m, are estimated according to the Reynolds number.

The model input parameters are mass flow rate, and inlet enthalpy for refrigerant; and volumetric flow rate and inlet temperature for the brine. The model outputs are evaporating pressure, outlet enthalpy for the refrigerant, outlet brine temperature, heat transfer areas dedicated to boiling and superheating as well as the cooling capacity.

4. Flow boiling correlations

The two-phase flow heat transfer coefficient of the refrigerant is one of the most important issues in the evaporator design. Available in the literature are different methods (or correlations) to calculate the flow boiling heat transfer coefficient. The final method selected will depend on the evaporator geometry, working fluid and predominant evaporation region.

There are different mechanisms to enhance heat transfer coefficient in evaporators [35]. Adding micro-fins to tubes of evaporators can produce thermal advantages (though pressure losses are incremented) [36]. As compared to smooth tubes, microfin tubes ensure a large heat transfer enhancement with a relatively low pressure drop increase and reduce the range of operating conditions leading to dry-out and partial dry-out. The presence of micro-fins may change the two-phase flow pattern and the relative importance of nucleate boiling and convective evaporation heat transfer mechanisms [37].

Diverse boiling flow heat transfer coefficient correlations for micro-fin tubes have been proposed in the past years. However, most of them have not been tested with experimental data using the considered mixtures. In this paper the models proposed by Koyama et al. [38], Yun et al. [39], and Akhavan-Behabadi et al. [40] are selected to analyse the model accuracy using R134a, R450A, R404A and R448A in the evaporator.

The Koyama et al. [38] adopted the Chen correlation, presenting a superposition-type model that considers the enhancement effect of micro-fins on the convective heat transfer and the nucleate boiling component. It presented good results for R22, R134a and R123 at mass velocity from 200 to 400 kg m^{-2} s^{-1}, heat fluxes from 5 to 64 kW m^{-2} and reduced pressure from 0.07 to 0.24. Due to the great amount of equations, this micro-fin model is detailed in Table 5.

The Yun et al. [39] model implemented non-dimensional parameters accounting for heat transfer enhancement over smooth tubes and physical phenomena into the basic form of a smooth tube

Table 5
Equations used in the Koyama et al. correlation [38].

$\alpha_{TP}=\alpha_{nb}+\alpha_{cb}$

$\alpha_{cb}=0.028F^{1/0.8}\,\mathrm{Re}_l^{0.8}\,\mathrm{Pr}_l^{0.4}\left(\frac{k_l}{d_i}\right)$

$\mathrm{Re}_l=\frac{G(1-x)d_i}{\mu_l}$

$F=1+2\left(\frac{1}{X_{tt}}\right)^{-0.88}+0.8\left(\frac{1}{X_{tt}}\right)^{1.03}$

$\alpha_{nb}=K^{0.745}S\alpha_{pb}$

$K^{0.745}=\left(1+0.875\eta+0.518\eta^2-0.159\eta^3+0.7907\eta^4\right)^{-1}$

$\eta=\frac{\alpha_{cb}}{S\alpha_{pb}};\ S=\frac{1-\exp(-\xi)}{\xi};\ \xi=\frac{D_b\alpha_{cb}}{k_l}$

$D_b=1\times10^{-5}\left(\frac{\rho_l C_{p,l}T_{evap}}{\rho_v h_{lv}}\right)^{1.25}\left(\frac{2\sigma}{g(\rho_l-\rho_v)}\right)^{0.5}$

$\alpha_{pb}=579.6\left(\frac{k_l}{D_{be}}\right)\left(\frac{q''D_{be}}{k_lT_{evap}}\right)^{0.745}\left(\frac{\rho_l}{\rho_v}\right)^{0.581}\mathrm{Pr}_l^{0.533}$

$D_{be}=0.51\left(\frac{2\sigma}{g(\rho_l-\rho_v)}\right)^{0.5}$

Table 6
Coefficients used on the Yun et al. correlation [39].

Coefficient	C_1	C_2	C_3	C_4	C_5	C_6	C_7	C_8	C_9
Value	0.009622	0.1106	0.3814	7.685	0.51	–0.736	0.2045	0.7452	–0.1302

correlation. They used a great amount of experimental points to obtain the correlation agreement and the average deviation was –11.7%. The equations that represent this model are Eqns. (9–11):

$$\alpha_{TP} = \alpha_l \left[C_1 \mathrm{Bo}^{C_2} \left(\frac{P_{evap} d_i}{\sigma} \right)^{C_3} + C_4 \left(\frac{1}{X_{tt}} \right)^{C_5} \left(\frac{G \cdot e}{\mu_l} \right)^{C_6} \right] \mathrm{Re}_l^{C_7} \mathrm{Pr}_l^{C_8} \left(\frac{\delta}{e} \right)^{C_9} \quad (9)$$

$$\mathrm{Bo} = \frac{q''}{G h_{lv}} \quad (10)$$

$$\alpha_l = 0.023 \mathrm{Re}_l^{0.8} \mathrm{Pr}_l^{0.4} \left(\frac{k_l}{d_i} \right) \quad (11)$$

Finally, Akhavan-Behabadi et al. [40] developed a correlation based on their R134a experimental results, to predict the micro-fin HTC at four different mass velocities (53, 80, 107 and 136 kg m^{-2} s^{-1}) and tube inclinations (from –90° to +90°). They obtained good agreement between the correlation and experimental values (an error band of ±10%). In the case of a horizontal tube the correlation results in Eqns. (12) and (13) (Table 6).

$$\alpha_{TP} = 4.05 \times 10^{-3} \mathrm{Re}_l^{0.98} F_\alpha^{0.38} (1.55 - x)^{0.96} \left(\frac{\mathrm{Pr}_l}{X_{tt}} \right)^{1.09} \quad (12)$$

$$F_\alpha = \begin{cases} 1 & x \le 0.7 \\ 1 + 0.2 x^{1.2} \cos(15\pi/180) & x > 0.7 \end{cases} \quad (13)$$

Although they are not studied here, other micro-fin tube models can be found in literature as those developed by Thome et al. [41] and Cavallini et al. [42]. Thome's correlation was the first developed introducing the geometrical dimensions of micro-fins and it considers the aggrandizement of nucleate boiling and convective evaporation caused by micro-fins. The Cavallini's model considers heat transfer mechanisms: nucleate boiling, convective evaporation and capillarity.

5. Results and discussion

5.1. Model validation

In order to check the predictive ability of the three flow boiling heat transfer correlations used in the evaporator model, three operational parameters of the evaporator have been selected: evaporating pressure, two-phase overall heat transfer coefficient (UA_{TP} product) and cooling capacity. Thus, Table 7 provides a summary of the statistical analysis in order to check the evaporator simulation versus experimental data using all flow boiling

Table 7
Statistical analysis of selected parameters of the model and experimental results.

Refrigerant	Parameter	Correlation	$\bar{\omega}$	$\lvert\bar{\omega}\rvert$	θ	$\lambda_{10\%}$
R134a	P_{evap}	Koyama et al.	5.19%	7.43%	10.04%	82%
		Yun et al.	2.05%	5.28%	8.59%	82%
		Akhavan-Behabadi et al.	–2.58%	7.30%	7.61%	82%
	UA_{TP}	Koyama et al.	34.25%	34.53%	28.60%	18%
		Yun et al.	24.41%	24.41%	23.79%	18%
		Akhavan-Behabadi et al.	9.89%	14.84%	21.43%	59%
	$Q_{o,ref}$	Koyama et al.	0.90%	1.25%	1.61%	100%
		Yun et al.	0.56%	0.90%	1.48%	100%
		Akhavan-Behabadi et al.	–0.32%	1.25%	1.44%	100%
R450A	P_{evap}	Koyama et al.	13.20%	13.20%	6.96%	32%
		Yun et al.	8.98%	8.98%	4.35%	59%
		Akhavan-Behabadi et al.	2.98%	3.74%	3.62%	91%
	UA_{TP}	Koyama et al.	23.88%	24.29%	15.26%	18%
		Yun et al.	12.67%	13.51%	8.21%	32%
		Akhavan-Behabadi et al.	–0.64%	5.45%	6.85%	82%
	$Q_{o,ref}$	Koyama et al.	2.59%	2.60%	1.57%	100%
		Yun et al.	2.04%	2.04%	1.12%	100%
		Akhavan-Behabadi et al.	0.93%	1.03%	0.90%	100%
R404A	P_{evap}	Koyama et al.	18.25%	18.25%	7.72%	17%
		Yun et al.	11.83%	11.83%	4.26%	33%
		Akhavan-Behabadi et al.	7.70%	7.71%	3.95%	67%
	UA_{TP}	Koyama et al.	31.30%	31.30%	13.68%	4%
		Yun et al.	15.78%	15.82%	9.32%	25%
		Akhavan-Behabadi et al.	6.25%	7.53%	7.30%	79%
	$Q_{o,ref}$	Koyama et al.	4.02%	4.02%	1.78%	100%
		Yun et al.	3.28%	3.28%	1.31%	100%
		Akhavan-Behabadi et al.	2.41	2.41%	1.13%	100%
R448A	P_{evap}	Koyama et al.	14.35%	14.35%	7.59%	62%
		Yun et al.	9.42%	9.42%	5.49%	62%
		Akhavan-Behabadi et al.	2.68%	4.33%	5.35%	85%
	UA_{TP}	Koyama et al.	29.71%	29.96%	20.69%	54%
		Yun et al.	17.04%	17.47%	16.31%	54%
		Akhavan-Behabadi et al.	1.18%	10.89%	11.80%	46%
	$Q_{o,ref}$	Koyama et al.	2.27%	2.31%	1.59%	100%
		Yun et al.	1.76%	1.76%	1.27%	100%
		Akhavan-Behabadi et al.	0.731%	0.96%	1.10%	100%

correlation provided. To do so, Eqns. (14–17) [43] are used to quantify its individual error (Eq. 14), mean error (Eq. 15), absolute mean error (Eq. 16) and standard deviation (Eq. 17) for predicted evaporating pressure, UA_{TP} product and cooling capacity, respectively.

$$\omega_i = \frac{Model\ value - experimental\ value}{experimental\ value} \tag{14}$$

$$\bar{\omega} = \frac{1}{n}\sum_{i=1}^{n}\omega_i \tag{15}$$

$$|\bar{\omega}| = \frac{1}{n}\sum_{i=1}^{n}\omega_i \tag{16}$$

$$\theta = \sqrt{\frac{1}{n}\sum_{i=1}^{n}(\omega_i - \bar{\omega})^2} \tag{17}$$

Although R134a is studied in Mendoza-Miranda et al. [31], it is also displayed here to compare the results (pure refrigerant) with the performed using the other refrigerants (near-azeotrope and non-azeotrope mixtures). Moreover, all the correlations used in this paper were validated by their authors using R134a, so it could suggest the magnitude of the deviation for the other refrigerants.

Figs. 2–4 show comparisons of measured and predicted data for the four refrigerants tested (R134a, R404A, R448A, R450A) and the flow boiling heat transfer correlations for micro-fin tubes developed by Koyama et al. [38], Yun et al. [39] and Akhavan-Behabadi et al. [40]. Fig. 2a highlights the measured evaporating pressure for each refrigerant and all boiling heat transfer correlations. It can be seen that the results agree quite well, with 82% of the points predicted to an accuracy of ±10% using the three correlations studied. It appears that the model using the Akhavan-Behabadi et al. correlation slightly underpredicts the evaporating pressure for low-load conditions using R134a; however, prediction is still within the error bandwidth. Fig. 2b shows a similar trend for R450A; the results agree with 32%, 59% and 91% of the points predicted to an accuracy of ±10% using the Koyama et al., Yun et al. and Akhavan-Behabadi et al. correlations, respectively. The Koyama et al. and Yun et al. correlations overpredict the evaporating pressure when evaporating pressure increases; meanwhile the Akhavan-Behabadi et al. correlation shows a slight overprediction (compared with the first two correlations) when evaporating pressure increases. Similar results are obtained for R404A and R448A (Fig. 2c and d), highlighting that for high evaporating pressure using R404A the overprediction increases up to 13% using the Koyama et al. correlation, 9% with the Yun et al. correlation and 7.7% with the Akhavan-Behabadi et al. correlation.

Fig. 3 shows the comparison between the product of the two-phase overall heat transfer coefficient and heat transfer area (UA_{TP}) for each refrigerant. In this case, the points observed are more

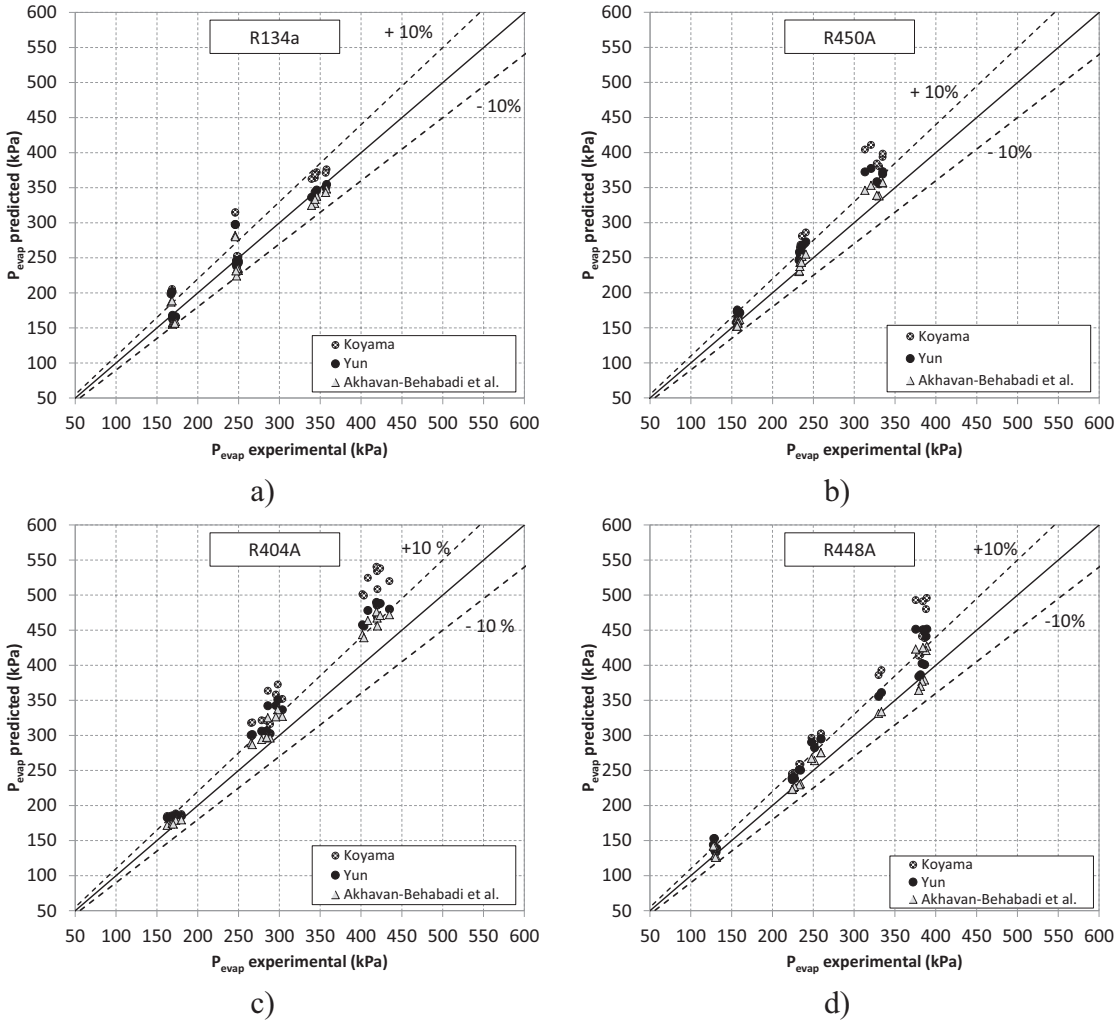

Fig. 2. Evaporating pressure model deviations for a) R134a, b) R450A, c) R404A and d) R448A.

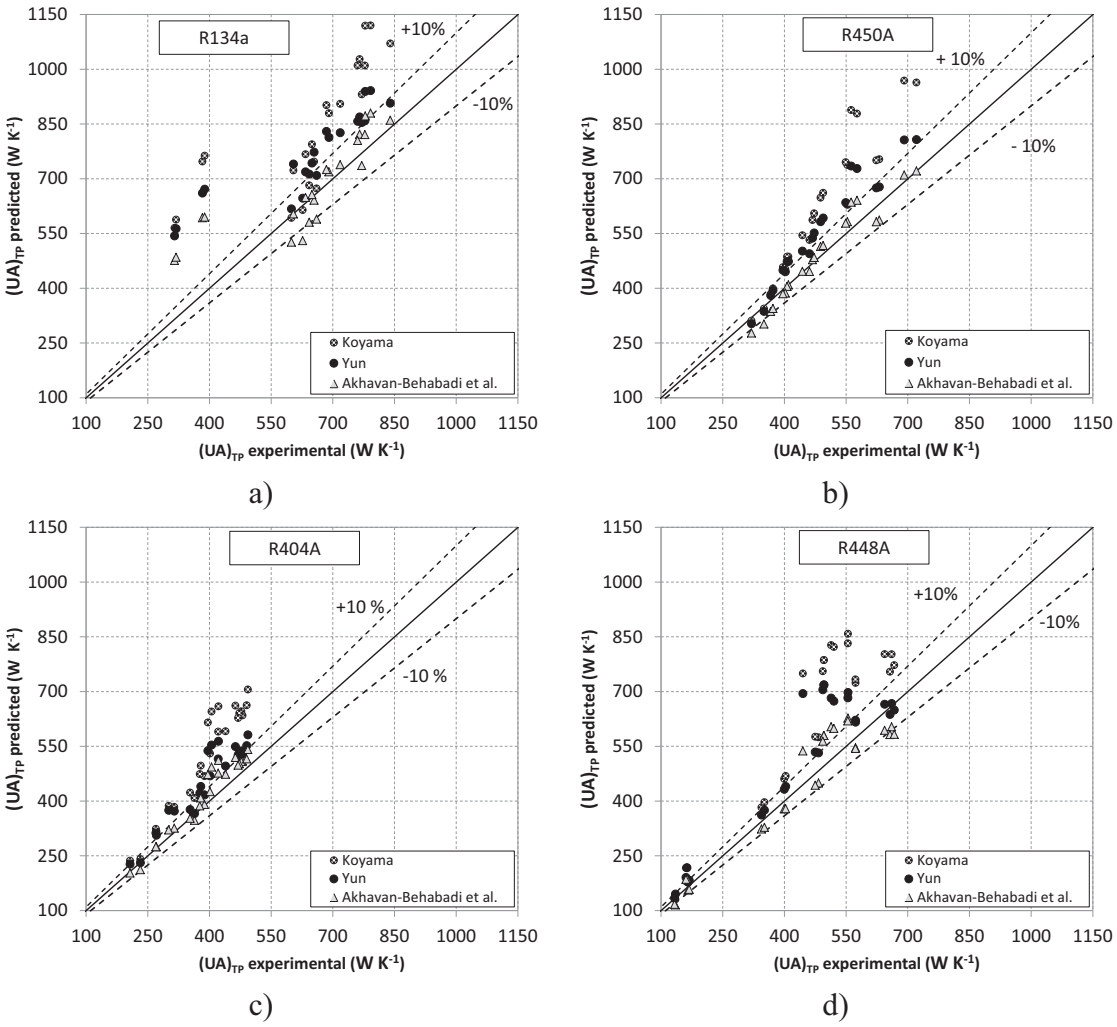

Fig. 3. UA_{TP} model deviations for a) R134a, b) R450A, c) R404A and d) R448A.

scattered than those observed in evaporating pressure. For the Koyama et al. and Yun et al. flow boiling correlations, the values are generally overpredicted, meanwhile for the Akhavan-Behabadi et al. correlation we obtained a best fit of our experimental data.

Finally, cooling capacity is the parameter that shows the most precise predictions, as all the values remain inside the ±10% error bandwidth, as shown in Fig. 4. Standard deviations are below 1.5% for all refrigerants using the Akhavan-Behabadi et al. correlation, and for the Koyama et al. correlation, the highest deviation obtained is 1.8% for R404A. The values are generally overpredicted except for R134a using the Akhavan-Behabadi et al. correlation. As observed before, the highest deviations are obtained at higher cooling capacities (same tests that higher evaporating pressures).

R450A is the first near-azeotrope mixture studied; as happens for R134a, values are overpredicted for all the correlations, the large deviation being that obtained with the Koyama et al. correlation. Intermediate deviation is obtained with the Yun et al. correlation and the correlation that best fits the experimental results is that of Akhavan-Behabadi et al. For p_{evap} and UA_{TP} almost the half of the values are within ±10%, being the high deviation at higher p_{evap}; additionally, all Q_{ref} predictions are inside the ±10% error bandwidth. On the other hand, similar results are obtained for the R448A zeotropic refrigerant mixture.

5.2. Evaporator performance

Once the evaporator model has been validated with the experimental results, this section compares the evaporator performance between the HFCs selected and their replacements. Because Akhavan-Behabadi et al. correlation provides the most precise predictions; the simulations have been performed applying this model. The comparison is performed at refrigerant mass flow rates between 0.025 and 0.09 kg s^{-1}. The input conditions of the comparison are indicated in Fig. 5, which shows the main results of the simulation.

The evaporating temperature (Fig. 5a) decreases with the increase in mass flow rate. In the case of R448A this evaporation temperature is lower due to the large glide effects that therefore is going to be reflected in a difference in evaporation pressure and compression ratio. The rest of the refrigerants display higher evaporation temperatures, being that of R404A the higher at high mass flow rates. Then, Fig. 5b presents the variation of the temperature of the brine at the evaporator inlet. It also presents a high difference between R404A and R448A due to the large R448A glide. Both, T_{evap} and T_{bse} will imply a very different pinch point between R404A and its alternative. The difference between R134a and R450A can be considered small, 0.6 K as average, mainly due to the R1234ze(E) inclusion in the mixture.

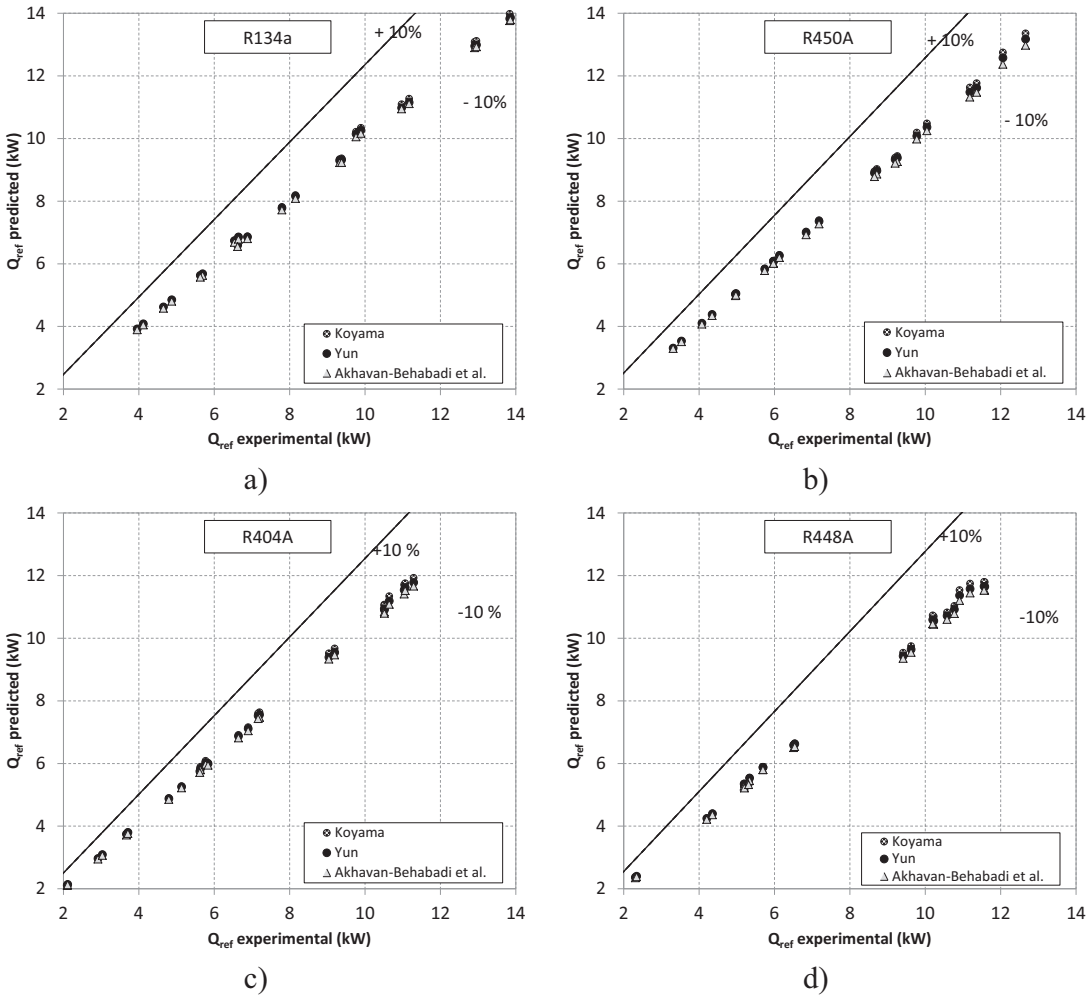

Fig. 4. Cooling capacity model deviations for a) R134a, b) R450A, c) R404A and d) R448A.

Fig. 5c represents the evaporator effectiveness at flow boiling, which is very similar for refrigerants R134a and R450A, and lies between 30 and 50% approximately. The effectiveness of R448A is above that performed by R404A, 5% as average, and indicates that the flow boiling HTC of both refrigerants are significantly different. Finally, the cooling capacity during evaporation of the fluids analyzed is shown in Fig. 5d. As the rest of parameters, R450A cooling capacity is very similar to that of R134a (especially at great mass flow rates). On the other hand, R448A cooling capacity is between 1.2 kW and 3.4 kW greater than that of R404A, affected directly by higher R448A evaporating enthalpy difference.

6. Conclusions

In this paper a micro-fin tube evaporator performance evaluation using two new low-GWP alternatives, R450A and R448A, and their baselines, R134a and R404A, was presented. The comparison was made using results obtained from a steady-state evaporator model. This model was validated using experimental measurements from a shell-and-micro-fin tube evaporator located in an experimental vapour compression system. Tests were carried out using various parameters such as evaporating pressure, mass flow rate or superheating degree, among others. The main conclusions of the work are summarized as follow.

The best predictions performed by the model are observed when the Akhavan-Behabadi et al. correlation is used, then the Yun et al. correlation and finally the Koyama et al. correlation. The use of the Akhavan-Behabadi et al. correlation allows obtainment of a great quantity of points inside the ±10% limits and lower mean error and standard deviation values. The deviation is low at lower evaporation temperatures (low mass flow rates and cooling capacity).

This micro-fin-tubes evaporator model performs accurate predictions for all refrigerants tested, for the higher precision of the model is observed for R450A and R404A (near-azeotropic mixtures), then R448A (azeotropic mixture) and finally R134a. The error observed is higher for UA_{TP} than evaporating pressure or cooling capacity, so this model is recommended to study operating conditions or evaporator energetic performance.

The evaporator performance of R450A is very similar to that of R134a, although it only presents 42% of R134a in its composition. Besides, R404A and R448A present a great difference for all parameters studied, mostly caused by glide effects, different HTCs and enthalpy difference.

Acknowledgements

The authors thankfully acknowledge “Ministerio de Educación, Cultura y Deporte” (Grant number FPU12/02841) for supporting this work through “Becas y Contratos de Formación de Profesorado Universitario del Programa Nacional de Formación de Recursos Humanos de Investigación del ejercicio 2012”. Finally the linguistic support of Irene I. Elías-Miranda is appreciated.

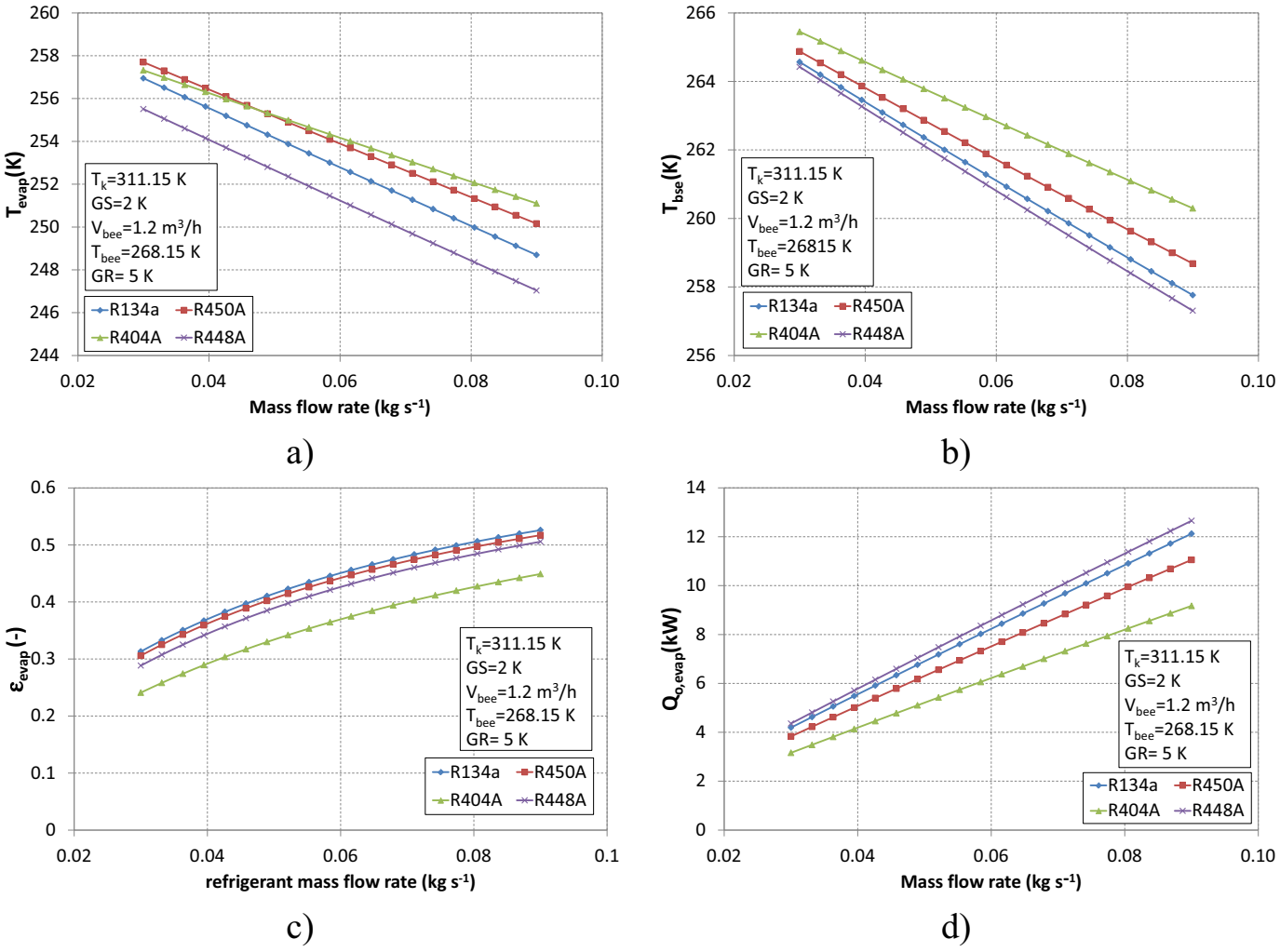

Fig. 5. Results of the simulation: a) evaporating temperature, b) temperature of the brine at the evaporator outlet, c) effectiveness at evaporating zone and d) cooling capacity.

Nomenclature

A	Heat transfer area (m^2)
Bo	Boiling number
C	Constant
C_p	Specific heat capacity (J kg^{-1} K^{-1})
d	Diameter (m)
e	Fin height (m)
g	Gravitational acceleration (m s^{-2})
G	Mass velocity (kg m^{-2} s^{-1})
GR	Subcooling degree (K)
GS	Superheating degree (K)
h	Specific enthalpy (J kg^{-1})
k	Thermal conductivity (W m^{-1} K^{-1})
n	Number of experimental data
NTU	Number of heat transfer units
P	Pressure (kPa)
Pr	Prandtl number
$\dot{Q}$	Thermal power (W)
q″	Heat flux (W m^{-2})
Re	Reynolds number
T	Temperature (K)
U	Overall HTC (W m^{-2} K^{-1})
$\dot{V}$	Volumetric flow rate (m^3 h^{-1})
x	Vapor quality
X_{tt}	Martinelli parameter

Greek symbols

α	Heat transfer coefficient (W m^{-2} K^{-1})
δ	Liquid film thickness (m)
ε	Effectiveness
μ	Dynamic viscosity (Pa s^{-1})
θ	Standard deviation
ρ	Density (kg m^{-3})
σ	Surface tension (N m^{-1})
ω	Mean error
$\lvert\bar{\omega}\rvert$	Absolute mean error

Subscripts

bee	Brine at the inlet
bse	Brine at the outlet
cb	Convective boiling
evap	Evaporator
i	Inlet
k	Condenser
l	Liquid
lv	Liquid–vapor
nb	Nucleate boiling

References

[1] E. Halimic, D. Ross, B. Agnew, A. Anderson, I. Potts, A comparison of the operating performance of alternative refrigerants, Appl. Therm. Eng. 23 (2003) 1441–1451.

[2] A. da Silva, E.P. Bandarra Filho, A.H. Pontes Antunes, Comparison of a R744 cascade refrigeration system with R404A and R22 conventional systems for supermarkets, Appl. Therm. Eng. 41 (2012) 30–35.

[3] K. Protocol, Report of the Conference of the Parties, United Nations Framework Convention on Climate Change (UNFCCC), 1997.

[4] The European Parliament and the Council of the European Union, Directive 2006/40/EC of The European Parliament and of the Council of 17 May 2006 relating to emissions from air-conditioning systems in motor vehicles and amending Council Directive 70/156/EC, Off. J. Eur Union 161 (2006) 12–18.

[5] The European Parliament and the Council of the European Union, Regulation (EU) No 517/2014 of the European Parliament and the Council of 16 April 2014 on fluorinated greenhouse gases and repealing Regulation (EC) No 842/2006, Off. J. Eur Union 150 (2014) 195–230.

[6] A. Mota-Babiloni, J. Navarro-Esbrí, Á. Barragán-Cervera, F. Molés, B. Peris, G. Verdú, Commercial refrigeration – an overview of current status, Int. J. Refrig. 57 (2015) 186–196.

[7] F. Molés, J. Navarro-Esbrí, B. Peris, A. Mota-Babiloni, Á. Barragán-Cervera, Theoretical energy performance evaluation of different single stage vapour compression refrigeration configurations using R1234yf and R1234ze(E) as working fluids, Int. J. Refrig. 44 (2014) 141–150.

[8] B. Minor, M. Spatz, A Low GWP Refrigerant for MAC, in: 2nd International Workshop on Mobile Air Conditioning and Auxiliary Systems, Torino, Italy, 2007.

[9] Honeywell International Inc, Solstice™ ze (HFO-1234ze) Refrigerant. The environmental alternative to traditional refrigerants, <http://www.honeywell-refrigerants.com/india/?document=solstice-ze-hfo-1234ze-brochure-2012&download=1>, 2012 (accessed 27.10.14).

[10] M. Koban, Automotive material investigation with low GWP refrigerant HFO-1234yf, in: Vehicle Thermal Management Systems Conference and Exhibition (VTMS10), Nottingham, United Kingdom, 2011.

[11] K. Schultz, S. Kujak, Low GWP AREP R134a W/C Screw Chiller Test Summary – Final Report, Air-Conditioning, Heating, and Refrigeration Institute (AHRI) Low-GWP Alternative Refrigerants Evaluation Program (Low-GWP AREP), Test Report #7, 2012.

[12] S. Fukuda, C. Kondou, N. Takata, S. Koyama, Low GWP refrigerants R1234ze(E) and R1234ze(Z) for high temperature heat pumps, Int. J. Refrig. 40 (2014) 161–173.

[13] A. Mota-Babiloni, J. Navarro-Esbrí, Á. Barragán, F. Molés, B. Peris, Drop-in energy performance evaluation of R1234yf and R1234ze(E) in a vapour compression system as R134a replacements, Appl. Therm. Eng. 71 (2014) 259–265.

[14] S. Kondo, K. Takizawa, K. Tokuhashi, Flammability limits of binary mixtures of ammonia with HFO-1234yf, HFO-1234ze, HFC-134a, and HFC-125, J. Fluorine Chem. 149 (2013) 18–23.

[15] A. Mota-Babiloni, J. Navarro-Esbrí, Á. Barragán-Cervera, F. Molés, B. Peris, Analysis based on EU Regulation No 517/2014 of new HFC/HFO mixtures as alternatives of high GWP refrigerants in refrigeration and HVAC systems, Int. J. Refrig. 52 (2015) 21–31.

[16] Honeywell, Solstice family of HFOs, <http://www.racplus.com/Journals/2012/06/01/g/s/r/Honeywell-presentation.pdf>, 2013 (accessed 5.06.14).

[17] A. Mota-Babiloni, J. Navarro-Esbrí, Á. Barragán-Cervera, F. Molés, B. Peris, Experimental study of an R1234ze(E)/R134a mixture (R450A) as R134a replacement, Int. J. Refrig. 51 (2015) 52–58.

[18] Tewis Smart Solutions, El rigor y metodología demuestran los beneficios del R450A* (Solstice® N13) en su carrera hacia un futuro, <http://www.tewis.com/newtewis/blog/descargas/Tewis_Mayo_14.pdf>, 2014 (accessed 12.04.15).

[19] Honeywell International Inc, Solstice® N13 (R-450A). Innovative Refrigeration System, Combining the 'Best of Both Worlds', <http://www.honeywell-refrigerants.com/europe/wp-content/uploads/2014/10/Case_Study_Groupe_Auchan_Solstice_N13_4pp_LR-140923.pdf>, 2014 (accessed 12.04.15).

[20] K. Schultz, S. Kujak, System Drop-In Tests of R134a Alternative Refrigerants (ARM-42a, N- 13a, N-13b, R-1234ze(E), and OpteonTM XP10) in a 230-RT Water-Cooled Water Chiller, Air-Conditioning, Heating, and Refrigeration Institute (AHRI) Low-GWP Alternative Refrigerants Evaluation Program (Low-GWP AREP), TEST REPORT #, 2013.

[21] Honeywell International Inc, Honeywell Solstice™ N40 Refrigerant Improved Energy Efficiency Case Study, Gaining Competitive Advantage through Improved Energy Efficiency and Reduced Environmental Impact, <http://www.honeywell-refrigerants.com/india/resources/customer-case-studies/honeywell-solstice-n40-improved-energy-efficiency-case-study/>, 2012 (accessed 25.03.14).

[22] A. Mota-Babiloni, J. Navarro-Esbrí, Á. Barragán, F. Molés, B. Peris, Theoretical comparison of low GWP alternatives for different refrigeration configurations taking R404A as baseline, Int. J. Refrig. 44 (2014) 81–90.

[23] S.F. Yana Motta, M.W. Spatz, G. Pottker, G.L. Smith, "Refrigerants with Low Environmental Impact for Refrigeration Applications", International Refrigeration and Air Conditioning Conference, 1554, <http://docs.lib.purdue.edu/iracc/1554>, 2014 (accessed 12.04.15).

[24] R. Rajendran, Promising Lower GWP Refrigerants in Air-Conditioning and Refrigeration Systems, Advancing Ozone & Climate Protection Technologies: Next Steps – Second International Conference (UNEP), Emerson Climate Technologies, Bangkok, 2013.

[25] O. Abdelaziz, B. Fricke, Working Fluids: Low Global Warming Potential Refrigerants, 2014 Building Technologies Office Peer Review – US Department of Energy, Oak Ridge National Laboratory, Arlington, VA, 2014.

[26] I. Dinçer, M. Kanoglu, Refrigeration Systems and Applications (Second Edition), John Wiley & Sons Ltd, Chichester, United Kingdom, 2010.

[27] R.W. Serth, T.G. Lestina, 9 – Boiling heat transfer, in: Process Heat Transfer (Second Edition), Academic Press, Boston, 2014, pp. 317–360.

[28] J. Navarro-Esbrí, F. Molés, Á. Barragán, A. Mota-Babiloni, J.M. Mendoza-Miranda, J.M. Belman, Shell-and-tube evaporator model performance with different two-phase flow heat transfer correlations. Experimental analysis using R134a and R1234yf, Appl. Therm. Eng. 62 (2014) 80–89.

[29] Y. Zhao, Y. Liang, Y. Sun, J. Chen, Development of a mini-channel evaporator model using R1234yf as working fluid, Int. J. Refrig. 35 (2012) 2166–2178.

[30] E.W. Lemmon, M.L. McLinden, Reference fluid thermodynamic and transport properties (REFPROP), version 9.1, in: NIST Standard Reference Database 23, Gaithersburg, MD, 2014.

[31] J.M. Mendoza-Miranda, J.J. Ramírez-Minguela, V.D. Muñoz-Carpio, J. Navarro-Esbrí, Development and validation of a micro-fin tubes evaporator model using R134a and R1234yf as working fluids, Int. J. Refrig. 50 (2015) 32–43.

[32] M. Jensen, A. Vlakancic, Technical note – experimental investigation of turbulent heat transfer and fluid flow in internally finned tubes, Int. J. Heat Mass Transfer 42 (1999) 1343–1351.

[33] V. Gnielinski, New equations for heat and mass transfer in turbulent pipe and channel flow, Int. Chem. Eng. 16 (1976) 359–368.

[34] A. Zhukauskas, Heat transfer from tubes in cross flow, in: J.P. Hartnett, T.F. Irvine (Eds.), Adv. in Heat Transf, vol. 8, Academic Press, New York, 1972.

[35] M. Siddique, A.-R.A. Khaled, N.I. Abdulhafiz, A.Y. Boukhary, Recent advances in heat transfer enhancements: a review report international, J. Chem. Eng. 2010 (2010) Article ID 106461 (28 pages).

[36] B. Sundén, V.V. Wadekar, W. Li, Heat transfer correlations for single-phase flow, condensation, and boiling in microfin tubes, Heat Transfer Eng. 36 (6) (2015) 582–595.

[37] A. Padovan, D. Del Col, L. Rossetto, Experimental study on flow boiling of R134a and R410A in a horizontal microfin tube at high saturation temperatures, Appl. Therm. Eng. 31 (2011) 3814–3826.

[38] S. Koyama, J. Yu, S. Momoki, T. Fujii, H. Honda, Forced convective flow boiling heat transfer of pure refrigerants inside a horizontal microfin tube, in: Proc. of the Convective Flow Boiling, Alberta, 1995.

[39] R. Yun, Y. Kim, K. Seo, H.Y. Kim, A generalized correlation for evaporation heat transfer of refrigerants in micro-fin tubes, Int. J. Heat Mass Transfer 45 (2002) 2003–2010.

[40] M.A. Akhavan-Behabadi, S.G. Mohseni, S.M. Razavinasab, Evaporation heat transfer of R-134a inside a microfin tube with different tube inclinations, Exp. Therm. Fluid Sci. 35 (2011) 996–1001.

[41] J.R. Thome, N. Kattan, D. Favrat, Evaporation in microfin tubes: a generalized prediction model, in: Proc. of Convect. Flow and Pool Boiling Conf., Irsee, Germany, 1997.

[42] A. Cavallini, D. Del Col, L. Rosseto, Flow boiling inside microfin tubes: prediction of the heat transfer coefficient, in: Proc. of ECI International, Spoleto, Italy, 2006.

[43] G. Bohm, G. Zech, Introduction to Statistics and Data Analysis for Physicists (First Edition), Deutsches Elektronen-Synchrotron, Hamburg, Germany, 2010.